Influence of Concentration and Anion Size on Hydration of H+ Ions and Water Structure

ARTICLE *in* THE JOURNAL OF PHYSICAL CHEMISTRY B · OCTOBER 2008

Impact Factor: 3.3 · DOI: 10.1021/jp805220j · Source: PubMed

Influence of Concentration and Anion Size on Hydration of H^+ Ions and Water Structure†

R. Mancinelli, A. Sodo, F. Bruni, and M. A. Ricci*

Dipartimento di Fisica "E. Amaldi", Università degli Studi "Roma Tre", Via della Vasca Navale 84, 00146 Roma, Italy

A. K. Soper‡

ISIS Facility, Rutherford Appleton Laboratory, Harwell Science and Innovation Campus, Didcot, Oxfordshire, OX11 0QX United Kingdom

Received: June 13, 2008; Revised Manuscript Received: July 22, 2008

Neutron diffraction experiments with hydrogen isotope substitution on aqueous solutions of HCl and HBr have been performed at concentrations ranging from 1:17 to 1:83 solute per water molecules, at ambient conditions. Data are analyzed using the empirical potential structure refinement technique in order to extract information on both the ion hydration shells and the microscopic structure of the solvent. It is found that the influence of these solutes on the water structure is less concentration dependent than that of salts or hydroxides. Moreover protons readily form a strong H-bond with a water molecule upon solvation, at all proportions. The majority of them is also bonded via a longer bond to another water molecule, giving a prepeak in the g_{OwOw}. At high solute concentration, the second water molecule may be substituted by the counterion. In particular at solute concentrations of the order of 1:17 or higher, all protons have an anion within a distance of 4.5 Å.

I. Introduction

The abnormal diffusion of water ions, namely H^+ and OH^-, in water[1,2] is currently rationalized as a Grotthus process, or structural diffusion as opposed to the mass diffusion process, or Stokes diffusion, undergone by all other ions in solution. This process is governed by thermally assisted proton transfer between two water molecules along an hydrogen bond (H-bond); consequently the local structure around the ion and how well this fits into the extended H-bond network is one of the key issues which may promote or limit the process. Concerning this point we have seen an intense debate in the literature on whether hydronium ions (H_3O^+) preferentially coordinate into Eigen ($H_9O_4^+$) or Zundel ($H_5O_2^+$) complexes.[3−16] On the other hand, recent ab initio simulations of an excess proton in water[7,16] have shown that both complexes are needed in order to describe the Grotthus process generated within the simulation, as the proton transfer proceeds via a structural fluctuation from an Eigen-like complex, through a Zundel-like one, to eventually form an Eigen-like complex with another water molecule.

Recent analysis of neutron diffraction data from a concentrated HCl aqueous solution[17] has highlighted the difficulty of making a clear distinction between Eigen and Zundel complexes, due to the continuous random network of H-bonds formed between water molecules and hydrated protons. In that work the experimental data have been analyzed through the empirical potential structure refinement code, (EPSR)[19,20] that is a Monte Carlo (MC) simulation, which equilibrates an ensemble of molecules in configurations compatible with the experimental data. In doing so three distinct hypothesis on the proton solvation have been considered: first that all protons form hydronium complexes, second that all of them form instead Zundel complexes, and third that the H^+ ions have been left free to equilibrate within the simulation box toward their preferred hydration shell. All three hypothesis allow fitting of the experimental data and give consistent results, but interestingly, it is not unusual to find Zundel-like complexes in the first simulation or Eigen-like in the second. Moreover the third simulation reveals that all protons readily form an H-bond with a water molecule, and a large amount of them are bonded to two water molecules: whether this hydrated proton could be called an Eigen or a Zundel complex is largely a question of definition, also in view of the large distortions of the structure of these complexes shown in the simulation and the high solute concentration considered at that time.

On the other hand experimental studies of proton hydration can only be performed by solvation of acids and consequently the counterion of an H^+ in these studies may be Cl^-, as in refs 11 and 17 or any other anion, but OH^-. This raises the question of the influence of the counterion on the hydronium solvation shell and on the solvent structure, as a function of the solute concentration. The latter issue, in particular, has been studied in a variety of aqueous solutions,[11,21−25] and the effect assimilated to that of an external pressure applied to pure water: a similarity that has been recently confirmed by molecular dynamics (MD) simulations as far as the dynamical properties of water in the presence of ions are concerned.[26]

Finally a study performed at different solute concentrations can elucidate the microscopic mechanism which limitates the equivalent conductance of these solutions at high concentration.[27,28]

Here we address the issues outlined above, by studying the microscopic structure of aqueous solutions of HCl and HBr as a function of solute concentration.

† Part of the special section "Aqueous Solutions and Their Interfaces".

* To whom correspondence should be addressed. E-mail: riccim@fis.uniroma3.it.

‡ Department of Physics and Astronomy, University College London, Gower Street, London WC1E 6BT, United Kingdom.

10.1021/jp805220j CCC: $40.75
Published on Web 09/23/2008

II. Experimental Details and Data Analysis

Neutron diffraction experiments with isotopic H/D substitution (NDIS) have been performed on HCl and HBr aqueous solutions, at concentration ranging from 1 solute per 83 water molecules to 1 solute per 17 water molecules, at standard temperature and pressure ($T = 298$ K, $p = 1$ bar). Measurements have been carried out at the SANDALS[29] diffractometer, installed at the ISIS Facility[30] (U.K.). Three samples, with different deuterium content (100%, 50%, and 0%) have been prepared by dilution from commercially available products.[31] Standard 1 mm Ti−Zr sample containers and the SANDALS sample changer connected to a water bath have been used. In addition to the measurement of the samples, data were collected on the background scattering, empty containers and vanadium sample, used for putting the data on an absolute scale of scattering cross section.

Diffraction data have been analyzed by using the Gudrun suite of programs, which performs corrections for multiple scattering, absorption and inelasticity effects, along with subtraction of the scattering from the sample container, and data reduction to an absolute scale.[32] The outputs of Gudrun are the three total neutron weighted interference differential cross sections (IDCS) defined as:

$$F(Q) = \Sigma_\alpha \Sigma_{\beta \geq \alpha} w_{\alpha\beta}[S_{\alpha\beta}(Q) - 1] \quad (1)$$

where Q is the exchanged wave-vector, α and β label the atomic sites, and

$$S_{\alpha\beta}(Q) = 4\pi\rho \int_0^\infty r^2 (g_{\alpha\beta}(r) - 1) \frac{\sin(Qr)}{(Qr)}\, dr \quad (2)$$

called partial structure factor (PSF), is the Fourier transform of the site−site radial distribution function (s-sRDF) $g_{\alpha\beta}(r)$ and ρ is the atomic number density of the solution in question. The individual PSF's are weighted in eq 1 by $w_{\alpha\beta} = c_\alpha c_\beta b_\alpha b_\beta (2 - \delta_{\alpha\beta})$, where c_α and c_β are the concentration of the α and β nuclei, and b_α and b_β are their scattering lengths,[33] respectively. Thus each experimental IDCS is a linear combination of 10 PSF, if we assume that after acid solution the H^+ ion can be considered distinct from water protons, although exchangeable with these. Consequently, in order to extract from three experimental data information on the hydration shells of both H^+ and the anion, A^-, and on the influence of these ions on the water−water correlations, direct Fourier transform of the IDCS or of combinations of the experimental data is of limited usefulness. We have instead used a simulation assisted procedure that has been developed in the past decade in order to convert IDCS data to real space, with extraction of the whole set of s-sRDF's. This is called empirical potential structure refinement (EPSR)[18−20] and is similar in principle to the methods routinely used in crystallography, which attempt to systematically refine a structural model of the diffraction data to give overall agreement with these. It goes without saying that the reliability of the individual simulated s-sRDF depends on its weight, $w_{\alpha\beta}$, reported in Table 1 for selected deuterated solutions. In the present experiment, where the isotopic substitution has been applied only on the hydrogen sites, water−water correlations and ions hydration shells are indeed more reliable than ion−ion s-sRDFs.

The EPSR method builds a simulation box with the same density and composition as the real sample. It does this by means of a reference interaction potential, U_{ref}, which incorporates the distinctive characteristics of the system in question (such as for instance the presence of H bonds), and is used to seed a MC simulation. Once it has reached equilibrium, a perturbation to the reference potential, called the empirical potential, derived directly from the diffraction data, is introduced and used to drive the simulated diffraction patterns as close as possible to the measured data. Since the fit of diffraction data is derived directly from the pair correlation function, this empirical potential is by definition purely pairwise additive. The MC simulation proceeds using both the reference potential and the empirical potential to accept or reject moves, and the empirical potential is adjusted iteratively until the fit to the data cannot be improved further. This method allows calculation of structural quantities beyond the s-sRDF, as in any simulation work; it can also help to identify any systematic bias that may affect one or more data sets, when features in the data not compatible with physical configurations of molecules are found.

At each acid concentration, a simulation box has been prepared according to Table 2, in order to match the experimental density[34] and composition of the samples. Following ref 17, no a priori hypothesis on the solvation structure of the H^+ ions has been done. The simple point charge/extended (SPC/E)[35] model has been used as reference potential for water; the ion sites have been modeled as Lennard-Jones centers plus charges (see Table 3 for the parameters). In particular the parameters for the H^+ and Cl^- ions are the same used in ref 17, and those for Br^- have been assigned, according to ref 36, assuming that $\varepsilon_{Br} = \varepsilon_{Cl}$ and that $[\sigma_{Br}]_{HBr}/[\sigma_{Br}]_{KBr} = [\sigma_{Cl}]_{HCl}/$

TABLE 1: Weights $w_{\alpha\beta} = c_\alpha c_\beta b_\alpha b_\beta (2 - \delta_{\alpha\beta})$ of the Individual PSF in the IDCS of Solutions of HCl and HBr in D_2O at Two Concentrations, Given As Number of Solute Molecules:Number of Solvent Molecules

1:17	O	D	D^+	Cl^-
O	3.4646	15.9312	0.4686	0.6727
D		18.3142	1.0773	1.5466
D^+			0.0158	0.0455
Cl^-				0.0327
1:83	O	D	D^+	Cl^-
O	3.682	16.93	0.1020	0.01464
D		19.46	0.2345	0.3367
D^+			0.0007	0.0020
Cl^-				0.0015
1:83	O	D	D^+	Br^-
O	3.682	16.93	0.1020	0.1039
D		19.46	0.2345	0.2389
D^+			0.0007	0.0014
Br^-				0.0007

TABLE 2: Details of the Simulation Boxes[a]

	c	m (mol/Kg)	L (Å)	N_w	N_s
HCl	1:17	3.3	29.84	830	50
	1:38	1.5	30.90	955	25
	1:83	0.7	28.22	738	9
HBr	1:17	3.3	30.26	850	50
	1:83	0.7	29.21	813	10

[a] L is the box length, N_w is the number of water molecules, and N_s is the number of HA couples.

TABLE 3: Parameters of the Reference Potential

	ϵ (kJ/mol)	σ (Å)	M	q (e)
O	0.65	3.166	16	−0.8476
H	0	0	2	0.4238
H^+	0.0075	0	2	0.9
Cl^-	0.419	4.380	35.44	−0.9
Br^-	0.419	4.743	79.90	−0.9

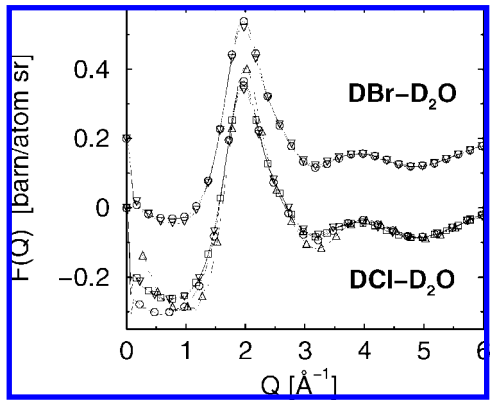

Figure 1. Experimental IDCS for the deuteriated samples at all studied concentrations (line plus symbol). Data for DBr solutions have been shifted for clarity. The correspondence of symbols to the solute: water proportions is the following: down triangle labels 1:83, squares 1:38, circles 1:17. In the case of DCl, also data from ref 17 are reported, as up triangles.

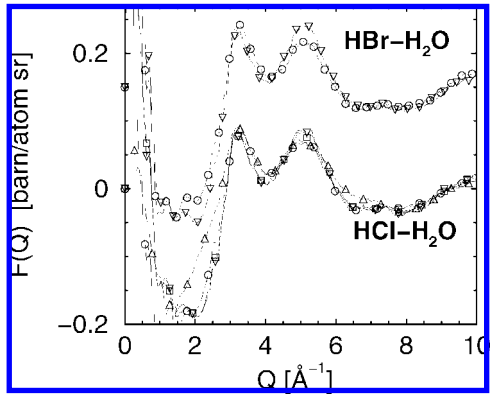

Figure 2. IDCS for the hydrogenated samples. Same symbols as in Figure 1.

$[\sigma_{Cl}]_{KCl}$. The Lorentz−Berthelot rules have been applied to describe the interaction between different atoms.

III. Discussion

In Figure 1 and 2, we report the IDCS data, for the deuteriated and hydrogenated samples, respectively, at all concentrations, including data for the 1:9 HCl solution of refs 11 and 17. As the solute concentration increases, the first peak of the $F(Q)$ function of the deuteriated samples moves to higher Q values and its minimum becomes more pronounced; at the same time the intensity of the first peak of the IDCS of the hydrogenated samples increases and that of the second one decreases. We notice that differences in the $F(Q)$ functions of molecular liquids are usually subtle and confined in the region below $Q = 10$ Å^{-1}, as in the present case. Given the low noise of the present data and their systematic trend with the solute concentration, we are confident about the reliability of the data refinement performed by using the Gudrun routine. These data have been further refined through the EPSR code, in order to transform the information from Q to r space, and we have checked that the trends shown by the data are correctly reproduced by the EPSR fits. In particular a good fit is achieved when the data-fit residuals are likely due to noise of the experimental data and residual systematic errors, such as a non perfect correction of the inelasticity contributions (particularly evident in the hydrogenated sample case below 1 Å^{-1}), and/or imperfect molecular geometry. The latter effect is indeed expected, due to the known

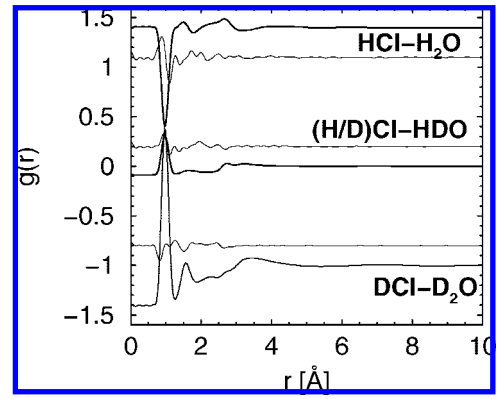

Figure 3. Neutron weighted $g(r)$ functions for the 1:17 solution of HCl, as calculated by the EPSR routine (thick solid line). The fit residuals are reported as a thin solid lines (shifted). Data for the deuteriated and hydrogenated sample have been shifted for clarity. The fit of the experimental data are all of the same quality.

differences between the geometries of an H_2O and a D_2O molecule, which are considered equivalent in our simulation box. The quality of the fit can then be better appreciated in r space, by comparing the total neutron weighted radial distribution functions, $g(r)$, of the three samples, obtained after accumulation of a large number (of the order of 3500) of MC configurations with their data-fit residuals (see Figure 3). When the fit is satisfactory, we expect that residual inelasticity effects, which are slow decaying functions in Q space, contribute to unphysical oscillations at r values shorter than the minimum approach distance. The imprecise "average" molecular geometry gives a misfit at the level of the intramolecular peaks; all the rest needs to be as unstructured as possible and reflects only the statistical noise of the data.[37,38]

A. Water−Water Correlations. The oxygen−oxygen RDF in pure water is characterized by two peaks at ∼2.8 and ∼4.5 Å that are considered the signature of the presence of an almost tetrahedral network of H-bonded molecules.[18] Solvation of electrolytes is known to disturb this network and traditionally ions have been classified as "structure breakers" or "structure makers", owing to their peculiar influence on the water−water network.[39,40] These definitions have been recently criticized,[25] and we will not discuss further this particular issue here. As a matter of fact, the effect of electrolytes solvation on the water network is visible as a shift of the peaks of the RDFs and in particular of the $g_{OwOw}(r)$, regardless of the structure maker/breaker definition of a particular ion: the extent of the deformation of the RDFs is instead specific of the ionic pair considered. It has been shown in previous work on aqueous electrolyte solutions that the most relevant effect of ions on the $g_{OwOw}(r)$ function is the shift of its second and third peak to shorter distances and this effect has been assimilated to that of an external pressure on the pure solvent.[11,21−25] Figure 4 shows that this same effect is visible in both HCl and HBr solutions but much less concentration dependent compared to the other solutions investigated. In particular at the lowest investigated concentration (1:83) NaCl and HCl solutions have quite similar $g_{OwOw}(r)$ functions, apart from the first peak (see the inset of Figure 4). In addition we notice in both acid solutions also a shift of the first peak to shorter distances at increasing solute concentrations, which was not observable in salt[25] or hydroxide solutions.[22−24] Particular attentions is due to a prepeak (also absent in salt solutions), which shows up at ∼2.3 Å and is due to the formation of complexes where two water molecules are bound through a H^+ bridge: we will see indeed, while discussing

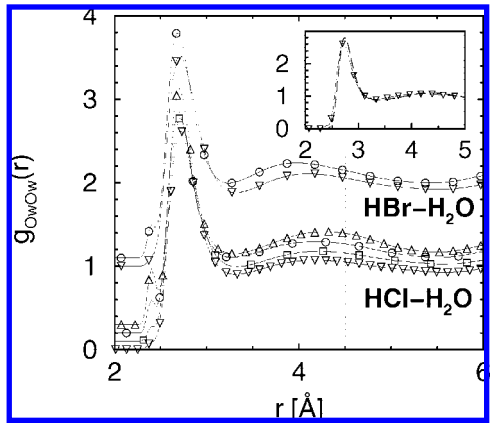

Figure 4. Radial distribution function of the water oxygens at all investigated concentrations of the two solutes. Same symbols as in Figure 1. The functions relative to HBr have been shifted up-words. Notice the presence of a prepeak and the shift of the first and second peak with increasing concentration. In the inset, the data for the 1:83 HCl solution are compared with those for a NaCl solution[25] at the same concentration (dashed line).

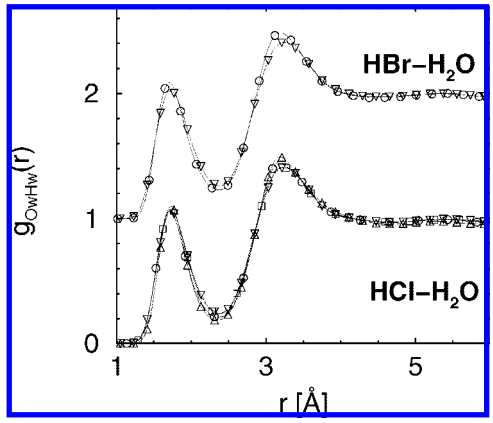

Figure 5. $g_{OwHw}(r)$ at all investigated concentrations. Same symbols as in Figure 1. Notice that the H-bond (first peak) is shorten than in pure water.

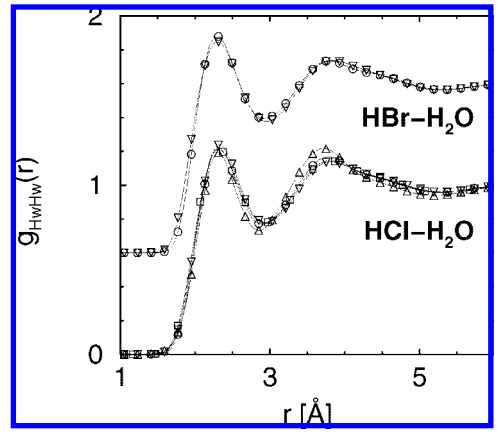

Figure 6. $g_{HwHw}(r)$ at all investigated concentrations. Same symbols as in Figure 1.

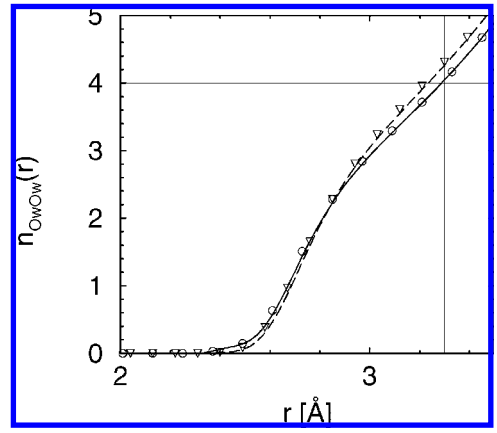

Figure 7. Running water oxygen's coordination numbers for HCl (solid and dashed line) and HBr (circles and down triangle) aqueous solutions at concentrations of 1 solute per 83 water molecules and 1 solute per 17 water molecules, respectively. These function is weakly concentration dependent and not sensibly depends on the solute.

the H^+ hydration, that this ion forms shorter H bonds with water oxygens, compared to those between two water molecules.The shortening of the first neighboring OwOw average distance matches with a shift to shorter distances of the first peak of the $g_{OwHw}(r)$ function (see Figure 5), compared to pure ambient water. This peak, that is traditionally called the H-bond peak, appears at $r \sim 1.73$ Å (instead of $r \sim 1.8$ Å in pure water) and moves to shorter distances with increasing the ion concentration. A similar trend is observed for the second peak of both this RDF and of the $g_{HwHw}(r)$ function (see Figure 6). All of these changes are substantially independent of the anion, as confirmed by the behavior of the running coordination number, $n_{OwOw}(r) = 4\pi\rho_{Ow} \int_0 g_{OwOw}(r)r^2\, dr$, reported in Figure 7. This function yields a number of first neighbor water molecules of the order of four in all samples, with a weak dependence on the solute concentration: it can be appreciated indeed that at the highest concentration the coordination number for the first water shell is lower than that found at the lowest, while the number of short contacts due to the prepeak of the $g_{OwOw}(r)$ increases with concentration.

B. Anion Hydration Shell. Looking at the anion hydration shell (see Figure 8), besides the trivial differences due to the different ionic size, we notice the same overall shape of both $g_{OwA}(r)$ and $g_{HwA}(r)$ functions. In particular the $g_{OwA}(r)$ suggests the presence at all concentrations of a well defined first neighbor shell, while the second shell becomes progressively less defined with increasing ion concentration. The $g_{HwA}(r)$ functions show an intense first peak, due to Hw-A bridges, as suggested by its distance from the first peak of the $g_{OwA}(r)$ functions (~0.9 Å). Interestingly in all $g_{OwA}(r)$ functions a prepeak develops with increasing solute concentration. This peak is at ~2.85 and ~3 Å in the case of HCl and HBr, respectively, and can be ascribed to Ow-H^+-A complexes. Notably, while the number of first neighbor oxygens (i.e., within a distance of 3.9 Å in the case of HCl and within 4.1 Å in the case of HBr) is between 6.5 and 7 at all concentrations, the number of first neighbor water hydrogens decreases with solute concentration from ~5.5 to ~5 at the highest concentration, where the number of H^+-A contacts increases. It is worth noting that the first peaks of the $g_{OwCl}(r)$ and $g_{HwCl}(r)$ functions are in these simulations shifted to slightly larger distances, compared to the case of NaCl and KCl solutions.[43] This may be due to the different Lennard-Jones parameters and charge used in this case for the reference potential model, and given the relatively low weight of these partial correlations in the experimental data, this difference has to be cautiously considered.

C. H^+ Hydration and Ion Contacts. As already mentioned in our simulation boxes, only H^+ ions have been allowed, in order to avoid a priori bias on the preferred hydration complexes. Moreover while analyzing the radial distribution functions of these ions and water atoms, it has to be born in mind that within the EPSR routine the water molecules are almost rigid. This

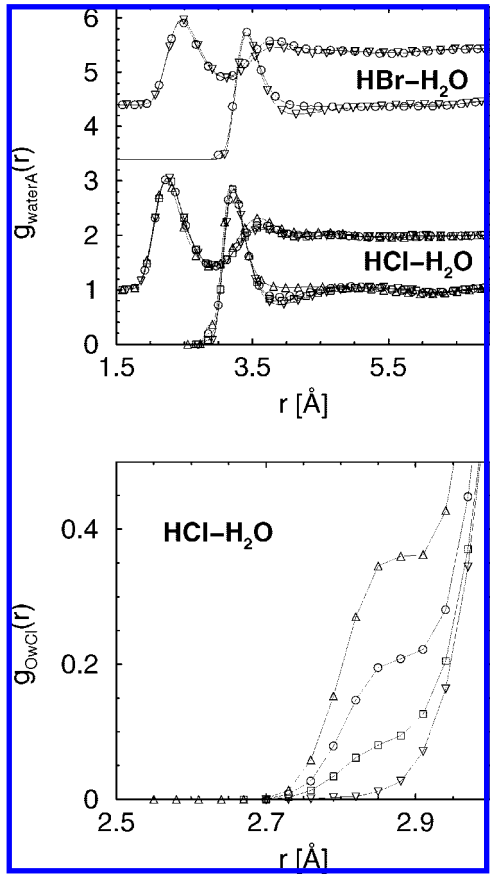

Figure 8. Top panel: The distribution functions of water atoms around the anion. Same symbols as in Figure 1 (data have been shifted for clarity). The short distance region of the $g_{OwCl}(r)$ function of the HCl solutions is shown in the bottom panel on a larger scale, in order to evidence the concentration dependence of the prepeak; the same behavior is visible in the $g_{OwBr}(r)$ function.

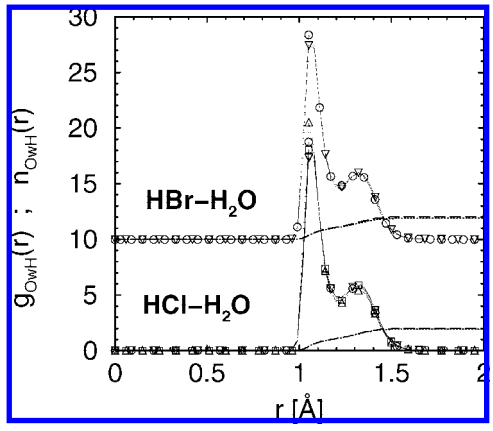

Figure 9. Short distance radial distribution function of the Ow-H^+ pair, showing two preferred first distances. Data for the HBr solution have been shifted by an arbitrary quantity for clarity and the same symbols as in Figure 1 have been used. The figure also reports the $n_{OwH}(r)$ functions at concentrations of 1:17 (dashed line) and 1:83 (dotted line).

implies that we will never find the signature of symmetric H_3O^+ ions, since this requires changing the Hw-Ow-Hw angle and moving the hydrogens out of plane. Nevertheless, it is evident in Figure 9 that at all concentration and independently on the anion the first peak of the $g_{OwH}(r)$ is double structured, because all H^+ ions form at least a very short bond (length ~1.05 Å) with a water molecule and the majority is also bonded to a

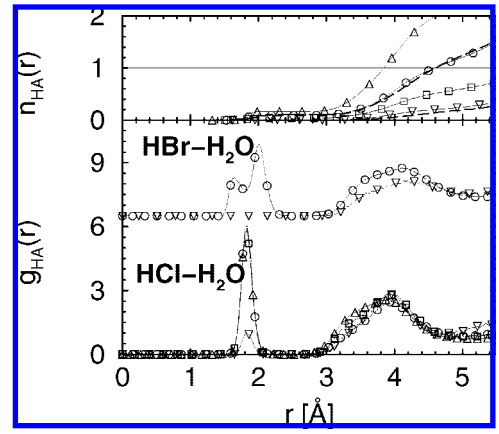

Figure 10. Bottom panel shows the short distance radial distribution function of the H-A pair. Data for the HBr solution have been shifted by an arbitrary quantity for clarity and the same symbols as in Figure 1 have been used. The top panel reports the running coordination numbers, $n_{HA}(r)$, (solid lines with symbols are used for the HCl solutions and dashed lines for the HBr ones), which exceed 1 at the end of the second peak, when the solute concentration is equal or higher than 1:17.

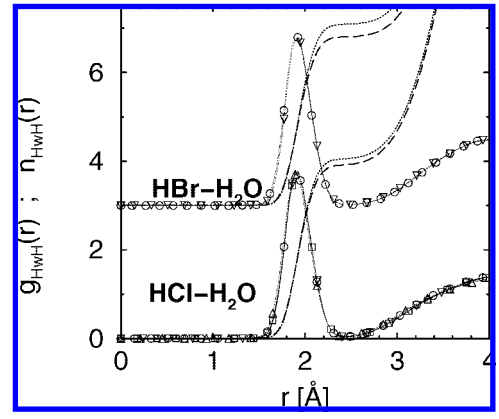

Figure 11. Short distance radial distribution function of the Hw-H^+ pair. Data for the HBr solution have been shifted by an arbitrary quantity for clarity and the same symbols as in Figure 1 have been used. The figure also reports the $n_{HwH}(r)$ functions at concentrations of 1:17 (dashed line) and 1:83 (dotted line).

second water molecule via a longer bond (length 1.33Å). Earlier results[17] are also reported in Figure 9, in order to show the weak concentration dependence of these correlation functions. As a matter of fact, with increasing acid concentration, the number of water molecules per H^+ ion available for the second bond decreases and the Ow-H^+-Ow bridge is sometimes replaced by an Ow-H^+-A bridge, as shown in Figure 10 where a peak due to direct ion contacts shows up at high concentrations. All the $g_{HwH}(r)$, reported in Figure 11, have a single first peak centered at ~1.9 Å: this result, although biased by the almost rigid molecular structure of water molecules in our simulation box, suggests that at least in the case of longer H bonds the three hydrogens of the complex cannot be coplanar with the oxygen. The number of hydrogens first neighbors of the H^+ ion are of the order of 4, consistently with the presence of 2 H-bonded water molecules: this number is weakly concentration dependent, in agreement with the finding that at high concentration a water molecule can be likely substituted by an anion, along the H-bond bridge.

Going back to Figure 10, we notice that the first peak of the $g_{HA}(r)$ function, due to direct ion contacts is absent or very weak at the lowest concentration. It is centered at ~1.85 Å in the

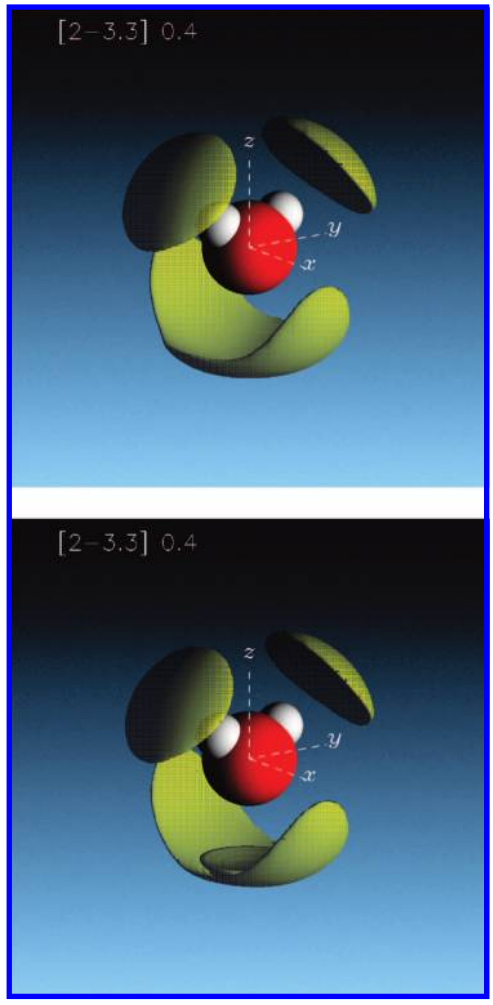

Figure 12. Spatial density functions of water molecules, whatever oriented, around a central molecule within the first neighbor shell distance, at concentrations of 1:83 (top panel) and 1:9 (bottom panel), in the case of HCl solutions. The isosurfaces of probability have been plotted for a contrast value of 0.4).

case of HCl solutions and shows two maxima (respectively at ~1.65 and ~2 Å) in the case of HBr at the highest solute concentration. These values compared with the bond length of the two molecules in the liquid phase, that is ~1.286[41] and ~1.446 Å,[42] respectively, tell us that although direct ion contact may occur, nevertheless the acids can still be considered dissociated. The broad second peak at ~4 Å is instead the signature of solvent separated ion pairs.

D. Further Structural Analysis. The availability of molecular configurations from the EPSR routine allows both a three-dimensional rendering of the orientational correlations between neighboring molecules and the analysis of structural properties, such as for instance the connectivity of the H-bond network, not otherwise available.

The first issue is tackled by evaluating, after spherical harmonic development of the s-sRDFs, the so-called spatial density functions (SDF).[44] These have been reported in Figure 12 in order to show the evolution with increasing solute concentration of the first neighbors shell around a water molecule. In correspondence of the hydrogen sites of the central molecule and of the lone pairs of its oxygen are indeed highlighted the isosurfaces of probability of finding another water molecule. The case of the 1:9 HCl solution, reported here in comparison with the lowest concentration, clearly shows the presence of a not negligible fraction of water molecules approaching closer to the oxygen site of the central one, compared to the rest. According to the analysis of the s-sRDFs reported in the previous sections, these molecules are sharing a H^+ bridge with the central one.

It is generally accepted that pure ambient water can be considered as a percolating H-bond network, which continuously reconstructs itself on the picosecond time scale of the H bonds.[45−48] This implies that if one calculates the distribution function of the water cluster size, $P(n)$, within a MC simulation box, it is expected that this function is peaked at a size value of the order of magnitude of the number of molecules within the box. This condition is fulfilled when the average number of H bonds per molecule exceeds the critical value, $n_c = 1.55$.[48] As a consequence also the present acidic solutions are expected to be a fully percolating system at all concentrations. This idea is confirmed by the analysis of the molecular configurations (data not shown), performed by adopting a geometrical definition of a H-bonded pair[49] and assuming that a group of molecules forms a cluster if each pair of molecules is bonded to at least one other molecule in the cluster. Moreover both H^+ and the anions present in these solutions form H bonds with water, thus bridging between different water clusters and enhancing the connectivity of the system, which plays a key role in the proton transfer mechanism. Nevertheless the equivalent conductance of these solutions decreases at very high acid concentration.[50] This can be rationalized as due to the presence of anions embedded into the network, which break the symmetry along the proton path. Evidence for this mechanism comes from Figure 10: this shows indeed that when the solute concentration is equal or higher than 1:17 the number of solvent separated ion contacts is equal to 1. Consequently, although the H-bond network is not dramatically distorted overall and the system is still percolating, the possible paths for H^+ transfer are limited by ion pairing in second shell.

IV. Conclusions

The first observation to be made is that changing the anion in these acid solutions has very little effect on the water−water correlations. Moreover comparing the $g_{OwOw}(r)$ obtained for NaCl solutions[25] with those reported here we notice that while the shift of the second peak at the lowest solute concentration is almost the same, in the case of acid solution the concentration dependence of this effect is very weak. We notice instead a shift to shorter distances of the first peak, which was not observed either in salt[25] or in hydroxide[22,23] solutions. These findings suggest that both H^+ and Cl^- or Br^- can fit quite easily into the H-bond network, avoiding dramatic distortions when the concentration increases. Indeed the H^+ can at most form two hydrogen bonds, connecting two water oxygens, as any water hydrogen, and since these are shorter than those between water molecules, on the average the distance between two water oxygens becomes shorter and a prepeak in the $g_{OwOw}(r)$ eventually develops at the higher concentrations. This contraction of the first solvation shell of the H^+ can at least partly contribute to the volume needed to solvate the anion. Cl^- and Br^- on the other hand are available for H-bonding with their first neighbor water molecules: the number of such bonds is higher than that between water molecules, due to the larger size and spherical symmetry of the anions, nevertheless these cannot impose their own symmetry and the ~5 H-bonded water molecules can accommodate the anion, without large distortions of their tetrahedral neighborhood.

As far as the H^+ hydration is concerned, present results confirm previous findings,[17] showing for both solutions that all

protons readily form a strong H-bond with a water molecule upon solvation. At low solute concentration all protons are also bonded via a longer bond to another water molecule, but when the solute concentration increases and ion contacts become more likely, the number of such bonds decreases, bringing along a reduction of the equivalent conductance[50] and proton mobility along the H-bond network. In particular the large number of solvent separated ion contacts found at solute concentrations of the order of 1:17 or higher may likely be responsible for this reduction.

Finally we mention that earlier data on HCl solutions obtained by neutron and X-rays diffraction[51] have been recently reanalyzed by reverse Monte Carlo[52] and our results are in fair agreement with the overall shape of the reported RDFs, although showing much less concentration dependence. Moreover a recent ab initio simulation study[53] shows good overall agreement with our results, even though a direct comparison in some cases cannot be performed, due to the different choice of the atomic sites used for the $g(r)$ definition, which is similar to that adopted in one of our previous work (see ref 11), where all hydrogens were considered to form hydronium ions. As a consequence our $g_{OwOw}(r)$ and $g_{OwCl}(r)$ are combinations of different radial distribution functions calculated in ref 53, in particular the first is a weighted sum of $g_{OO}(r)$, $g_{OOH_3^+}(r)$ (not shown in the paper) and $g_{OH_3^+OH_3^+}(r)$, and the second of $g_{OCl}(r)$ and $g_{OH_3^+Cl}(r)$. The observed prepeaks in Figures 4, 8 and 12 of our work can be indeed reasonably reproduced, by combining the data of ref 53 according to the procedure adopted in ref 17.

Acknowledgment. This work has been performed within the Agreement No. 01/9001 between CCLRC and CNR, concerning collaboration in scientific research at the spallation neutron source ISIS and with partial financial support of CNR.

References and Notes

(1) Robinson R. A.; Stokes R. H. *Electrolyte Solutions*, 2nd ed.; Butterworth: London, 1959.
(2) Atkins P. W. *Physical Chemistry zprint>,* 5th ed.; Freeman: New York, 1994.
(3) Wei, D.; Salahub, D. R. *J. Chem. Phys.* **1994**, *101*, 7633.
(4) Tuckerman, M.; Laasonen, L.; Sprik, M.; Parrinello, M. *J. Chem. Phys.* **1995**, *103*, 150.
(5) Tuckerman, M.; Laasonen, L.; Sprik, M.; Parrinello, M. *J. Phys. Chem.* **1995**, *99*, 5749.
(6) Agmon, N. *J. Phys. Chem. A* **1998**, *102*, 192.
(7) Marx, D.; Tuckerman, M. E.; Parrinello, M. *Nature* **1999**, *397*, 601.
(8) Schmitt, U. W.; Voth, G. A. *J. Chem. Phys.* **1999**, *111*, 9361.
(9) Geissler, P. L.; Dellago, C.; Chandler, D.; Hutter, J.; Parrinello, M. *Science* **2001**, *291*, 2121.
(10) Sillanpaa, A. J.; Laasonen, K. *Phys. Chem. Chem. Phys.* **2004**, *6*, 555.
(11) Botti, A.; Bruni, F.; Imberti, S.; Ricci, M. A.; Soper, A. K. *J. Chem. Phys.* **2004**, *121*, 7840.
(12) Astagiri, D.; Pratt, L. R.; Kress, J. D. *Proc. Natl. Acad. Sci.* **2005**, *102*, 6704.
(13) Headrick, J. M.; Diken, E. G.; Walters, R. S.; Hammer, N. I.; Christie, R. A.; Cui, J.; Myshakin, E. M.; Duncan, M. A.; Johnson, M. A.; Jordan, M. A. *Science* **2005**, *308*, 1765.
(14) Wang, F.; Voth, G. A. *J. Chem. Phys.* **2005**, *122*, 144105.
(15) Izvekov, S.; Voth, G. A. *J. Chem. Phys.* **2005**, *123*, 044505.
(16) Marx, D. *ChemPhysChem.* **2006**, *7*, 1848.
(17) Botti, A.; Bruni, F.; Ricci, M. A.; Soper, A. K. *J. Chem. Phys.* **2006**, *125*, 014508.
(18) Soper, A. K. *Chem. Phys.* **1996**, *202*, 295.
(19) Soper, A. K. *J. Mol. Liq.* **1998**, *78*, 179. Soper, A. K. *Chem. Phys.* **2000**, *258*, 121. Soper, A. K. *Mol. Phys.* **2001**, *99*, 1503.
(20) Soper, A. K. *Phys. Rev. B* **2005**, *72*, 104204.
(21) Leberman, R.; Soper, A. K. *Nature* **1995**, *378*, 364.
(22) Botti, A.; Bruni, F.; Imberti, S.; Ricci, M. A.; Soper, A. K. *J. Chem. Phys.* **2004**, *120*, 10154.
(23) Imberti, S.; Botti, A.; Bruni, F.; Cappa, G.; Ricci, M. A.; Soper, A. K. *J. Chem. Phys.* **2005**, *122*, 194509.
(24) McLain, S. E.; Imberti, S.; Soper, A. K.; Botti, A.; Bruni, F.; Ricci, M. A. *Phys. Rev. B* **2006**, *74*, 094201.
(25) Mancinelli, R.; Botti, A.; Bruni, F.; Ricci, M. A.; Soper, A. K. *Phys. Chem. Chem. Phys.* **2007**, *9*, 2959.
(26) Holzmann, J.; Ludwig, R.; Geiger, A.; Paschek, D. *Angew. Chem. Int.* **2007**, *46*, 8907.
(27) Debey, P.; Huckel, H. *Z. Phys.* **1924**, *25*, 49.
(28) Onsager, L. *Z. Phys.* **1926**, *27*, 388.
(29) (a) Onsager, L. *Z. Phys.* **1927**, *28*, 277. (b) SoperA. K., In *Proceedings of the Conference on Advanced Neutron Sources*; Hyer, D. K.; Institute of Physics and Physical Society: London, 1989; p 353; IOP Conf. Proc. no. 97. Detailed information on the SANDALS diffractometer can be also found at the web site: www.isis.rl.ac.uk.
(30) www.isis.rl.ac.uk.
(31) HCl/DCl 37% wt in H_2O or D_2O, respectively; HBr 48% wt in H_2O; DBr 47% wt in D_2O; from Sigma Aldrich.
(32) see: www.isis.rl.ac.uk/disordered/Sandals/ATLAS manual DTB.pdf.
(33) Sears, V. F. *Neutron News* **1992**, *3*, 26.
(34) Sohnel D.; Novotny P. In *Densitry of Aqueous Solutions of Inorganic Substances*; Elsevier: Amsterdam, 1985.
(35) Berendsen, H. J. C.; Grigera, J. R.; Straatsma, T. P. *J. Phys. Chem.* **1987**, *91*, 6269.
(36) Soper, A. K.; Weckstrom, K. *Biophys. Chem.* **2006**, *124*, 180.
(37) Soper A. K.; Benmore, C. J. *Phys. Rev. Lett.* **2008**, *101*, 065502.
(38) Bernabei, M.; Botti, A.; Bruni, F.; Ricci, M. A.; Soper, A. K. *Phys. Rev. E* **2008**, in press.
(39) Bernal, J. D.; Fowler, R. H. *J. Chem. Phys.* **1933**, *1*, 515.
(40) Hribar, B.; Southall, N. T.; Vlachy, V.; Dill, K. A. *J. Am. Chem. Soc.* **2002**, *124*, 12302.
(41) Powles, J. G.; Oran, E. K.; Dore, J. C.; Chieux, P. *Mol. Phys.* **1981**, *43*, 1051.
(42) Andreani, C.; Menzinger, F.; Ricci, M. A.; Soper, A. K.; Dreyer, J. *Phys. Rev. B* **1994**, *49*, 3811.
(43) Mancinelli, R.; Botti, A.; Bruni, F.; Ricci, M. A.; Soper, A. K. *J. Phys. Chem. B* **2007**, *111*, 13570.
(44) Svishchev, I. M.; Kusalik, P. G. *J. Chem. Phys.* **1993**, *99*, 3049.
(45) Stanley, H. E. *J. Phys. A: Math. Gen.* **1979**, *12*, L329.
(46) Stanley, H. E.; Teixeira, J. *J. Chem. Phys.* **1980**, *73*, 3404.
(47) Geiger, A. ; Stanley, H. E. *Phys. Rev. Lett.* **1982**, *49*, 1895.
(48) Blumberg, R. L.; Stanley, H. E.; Geiger, A.; Mausbach, P. *J. Chem. Phys.* **1984**, *80*, 5230.
(49) Two molecules are considered as H-bonded when the distance of a proton on one molecule to the oxygen of another is less than or equal to the position of the first minimum of the $g_{OwHw}(r)$.
(50) *CRC Handbook of Chemistry and Physics*, 82nd ed.; Lide, R., Ed.; CRC Press: Boca Raton, FL, 2001−2002.
(51) Triolo, R.; Narten, A. H. *J. Chem. Phys.* **1975**, *63*, 3624.
(52) Harsanyi, I.; Pusztai, L. *J. Phys.: Condensed Matter* **2005**, *17*, 859.
(53) Heuft, J. M.; Meijer, E. J. *Phys. Chem. Chem. Phys.* **2006**, *8*, 3116.

JP805220J